

# Diffuse Liver Disease: Cirrhosis, Focal Lesions in Cirrhosis, and Vascular Liver Disease

Khoschy Schawkat and Caecilia S. Reiner

## Learning Objectives

- To know MR techniques useful to quantify liver steatosis and fibrosis
- To recognize the characteristic and atypical contrast-enhancement pattern of hepatocellular carcinoma
- To discuss the MR imaging appearance of focal lesions in the cirrhotic liver and the use of the standardized reporting system LI-RADS
- To learn about HCC mimics and diffuse vascular liver disease causing liver parenchyma alteration

## 21.1 Cirrhosis

### 21.1.1 Imaging of Pre-stages of Cirrhosis

With the growing epidemics of diabetes, obesity, and metabolic syndrome, the prevalence of nonalcoholic fatty liver disease (NAFLD) is rising worldwide. NAFLD has become one of the most common causes of chronic liver disease. It is commonly classified into two phenotypes, nonalcoholic fatty liver (NAFL) and nonalcoholic steatohepatitis (NASH). The need for noninvasive screening and monitoring protocols with imaging as an alternative to liver biopsy to define therapeutic targets and treatment end points in NASH is emerging with growing burden of NAFLD. Significant advances in magnetic resonance imaging (MRI) allow quantification of

hepatic steatosis by measuring the proton-density fat fraction (PDFF) of MRI-visible protons bound to fat divided by all protons in the liver (bound to fat and water) with chemical shift imaging. The technique acquires multiple images at echo times optimally spaced for fat and water separation and T2\* signal decay correction. Several studies proved that MRI-PDFF is a robust, quantitative, accurate, and reproducible noninvasive biomarker for the assessment of NAFLD [1–4].

The next step in the cascade of diffuse liver disease is the development of liver fibrosis commonly on the basis of steatohepatitis or hepatitis B or C. Quantification of hepatic fibrosis is either possible with ultrasound (US)-based or MR elastography (MRE). MRE can be accomplished with most MR scanners by adding hardware to generate mechanical waves. Increased rigidity caused by collagen deposition can be visualized by modified phase-contrast pulse sequences. The stiffness generated from the wave propagation information can be depicted on cross-sectional elastogram images. Several studies have demonstrated a high diagnostic accuracy of MRE (AUC 0.90–0.98, 95% CI 0.84–0.94) for identifying clinically significant fibrosis (stage 2 or higher) (Fig. 21.1) with advantages of MRE over US-based elastography [5–9].

### 21.1.2 Imaging of Cirrhosis

Cirrhosis as a common endpoint of chronic liver disease is characterized by progressive fibrosis of the liver parenchyma with ongoing regeneration. Cirrhosis is most commonly the result of hepatitis B and C or chronic alcoholism; other causes are metabolic, biliary, and cryptogenic diseases. At an early stage of cirrhosis, the liver may appear normal. With disease progression, heterogeneity and surface nodularity are observed. Because of the unique ability of the liver to regenerate in cirrhosis, the liver harbors a spectrum of hepatocellular nodules, most of which are regenerative. Due to

K. Schawkat · C. S. Reiner (✉)  
 Institute of Diagnostic and Interventional Radiology,  
 University Hospital Zurich, Zurich, Switzerland  
 e-mail: [khoschy.schawkat@usz.ch](mailto:khoschy.schawkat@usz.ch); [caecilia.reiner@usz.ch](mailto:caecilia.reiner@usz.ch)

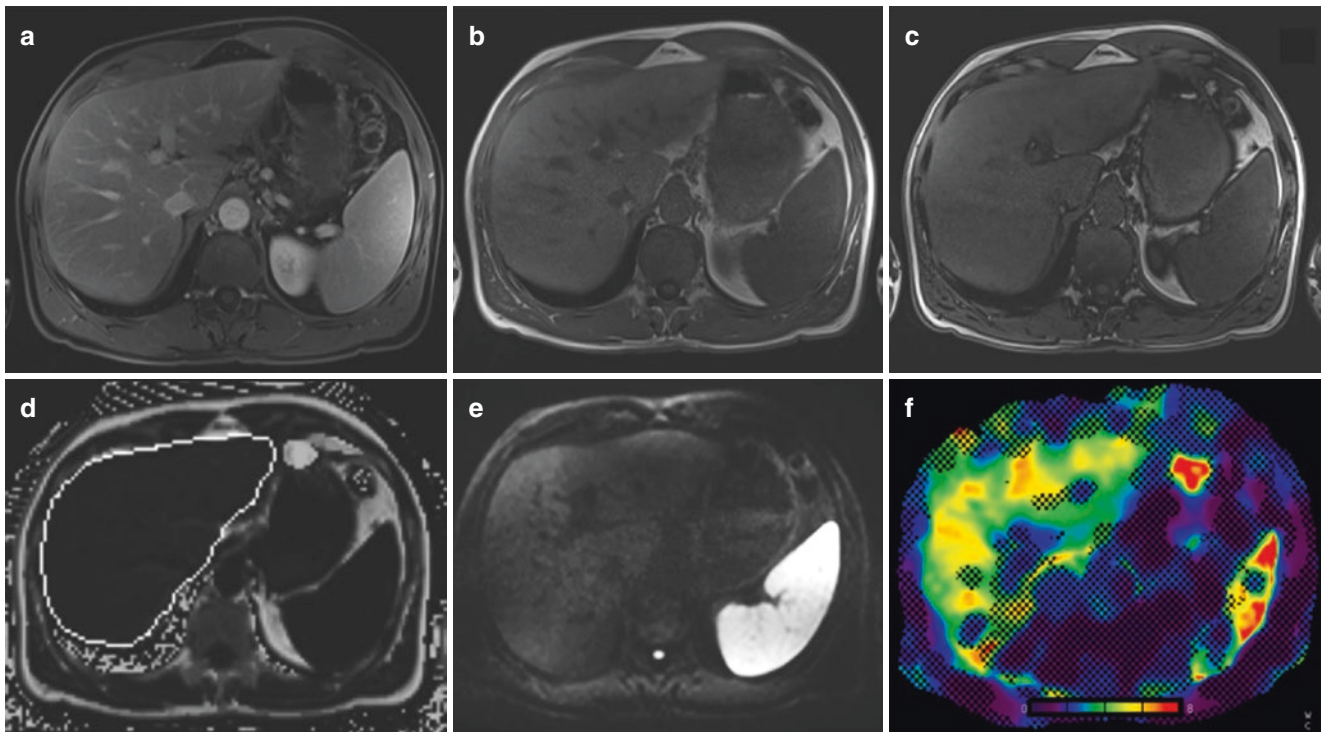


**Fig. 21.1** Imaging pre-stages of cirrhosis. 53-year-old male patient with chronic hepatitis C, genotype C. Histology proved moderate inflammatory activity (METAVIR A2) and portal fibrosis (METAVIR F3, Ishak 4). (a) Axial T1-weighted post-contrast magnetic resonance (MR) image in the portal venous phase does not show features of liver cirrhosis. No signal drop of the liver parenchyma is observed from the in-phase (b) to the out-of-phase gradient-dual-echo sequence (c).

(d) Axial proton-density fat fraction map from a gradient multi-echo sequence with automated liver segmentation showed normal liver fat content (mean  $\pm$  SD:  $5.0 \pm 0.8\%$ ). (e) Diffusion-weighted axial image with a b-value of  $800 \text{ s/mm}^2$  shows increased signal of the liver parenchyma. (f) Stiffness map from MR elastography demonstrated increased stiffness of  $4.9 \pm 0.6 \text{ kPa}$  corresponding to advanced fibrosis

the ongoing distortion of the liver parenchyma, the liver surface appears smooth, nodular, or lobular in most of the cases. Caudate lobe hypertrophy is the most characteristic morphologic feature of liver cirrhosis [10]. Alteration of blood flow results in typical morphologic abnormalities such as segmental hypertrophy involving the lateral segments of the left lobe (segment 2, 3) and segmental atrophy affecting the right lobe (segment 6, 7) and medial segment of the left lobe (segment 4). Other typical findings include enlargement of hilar periportal space, the right posterior notch sign, and generalized widening of the interlobar fissures. Less typical distribution of segmental atrophy and hypertrophy is seen in primary sclerosing cholangitis, where the distribution follows in part the distribution of the bile duct involvement, and, for example, atrophy of segments 2 and 3 or 5 and 7 may be seen. In 25% of cirrhosis, the liver shape and contour appears normal on CT or MRI.

Lymph adenopathy can appear in the liver hilum and peripancreatic region, which may mimic neoplastic lymph nodes, if the lymph nodes are large. Portal hypertension due to increased vascular resistance at the level of the hepatic sinusoids causes complications such as ascites and develop-

ment of portosystemic shunts at the lower end of the esophagus and at the gastric fundus, via periumbilical veins and left gastric vein. Other shunts include splenorenal collaterals, hemorrhoidal veins, and abdominal wall and retroperitoneal collaterals [10]. These collateral veins are seen as enhancing tortuous vessels. The typical nodular liver contour and liver shape of cirrhosis as well as its vascular complications can be seen on ultrasound, CT, or MRI. MRI very well depicts fibrotic bands between regenerative nodules as T2 hyperintense and progressively or delayed enhancing structures.

## 21.2 Focal Lesions in Cirrhotic Liver

### 21.2.1 Regenerative Nodules

Regenerative nodules are present in a cirrhotic hepatic environment surrounded by fibrous septa and result from continuous injury to the liver parenchyma resulting usually in cirrhosis. They play a role in the stepwise carcinogenesis of HCC, most frequently through dedifferentiation, which occurs in the following order: regenerative nodule, low-

grade dysplastic nodule, high-grade dysplastic nodule, and HCC. Most regenerative nodules do not progress in the dedifferentiation process. They are macronodular ( $\geq 9$  mm) or micronodular (3–9 mm). MR imaging demonstrates regenerative nodules with greater sensitivity than other imaging modalities; these nodules are visualized in only 25% of unenhanced CT scans and approximately in 50% of MR images [11]. Regenerative nodules are usually iso- to hypointense on T2-weighted images. Variable signal intensity on T1-weighted images is due to lipid, protein, or copper content leading to a T1-weighted hyperintense appearance or iron deposition in the so-called siderotic nodules leading to a hypointense appearance on T1-weighted images. The most usual appearance on T1-weighted images is isointense. Using extracellular gadolinium-containing contrast agent, regenerative nodules appear hypointense in the arterial and portal venous phase and isointense during equilibrium and delayed phases. After administration of hepatobiliary-specific contrast material, regenerative nodules enhance to the same degree as adjacent liver because they have normal hepatocellular and phagocytic functions [12].

### 21.2.2 Dysplastic Nodules

Dysplastic nodules are regenerative nodules that contain atypical hepatocytes, measuring at least 1 mm, not meeting histologic criteria for malignancy. They are classified as low- or high-grade dysplastic nodules. High-grade dysplastic nodules are considered premalignant and are characterized by moderate cytologic and architectural atypia to a degree insufficient to render a diagnosis of HCC. The differentiation between a regenerative nodule and a low-grade dysplastic nodule is difficult due to similar appearance on MRI with iso- to hypointense appearance on T2-weighted images and iso- or hyperintense appearance on T1-weighted images. Dysplastic nodules are rarely detected on CT. Dysplastic nodules usually are hypovascular and do not show hyperenhancement with extracellular contrast agents. In high-grade dysplastic nodules, arterial vascularization can increase leading to arterial hyperenhancement on imaging. Using hepatocyte-specific MR contrast agents, dysplastic nodules show variable signal intensity in the hepatocyte-specific phase. With progressing dedifferentiation, the nodules lose their ability to take up the hepatocyte-specific contrast agent (Gd-EOB-DTPA) and appear hypointense in the hepatobiliary phase. These hepatobiliary hypointense dysplastic nodules may be mistaken for HCC. Dysplastic nodules may also instead lose the ability to excrete the hepatocyte-specific contrast agent and appear iso- or hyperintense on hepatobiliary phase images. Hypovascular cirrhotic nodules with hypointense appearance in the hepatobiliary phase carry a significant risk of transforming into hypervascular HCC with

a pooled overall rate of 28% (95% CI, 22.7–33.6%). The size of the hypovascular nodule is a second risk factor for hypervascular transformation with nodules  $\geq 9$  mm in size showing a higher risk [13].

The earliest definitive sign of dysplastic nodule dedifferentiation is the “nodule within a nodule” appearance which is a dysplastic nodule harboring a focus of HCC, occurring in approximately 6% of patients with dysplastic nodules. However, it is believed that the majority of dysplastic nodules do not progress to an HCC.

### 21.2.3 Hepatocellular Carcinoma

Hepatocellular carcinoma (HCC) is the fifth most common cancer worldwide, and its incidence is rising occurring most frequently in patients with cirrhosis or chronic viral hepatitis. HCC occurs as a solitary lesion (in half of the cases) and as multiple lesions or diffuse. It differs from most malignancies because it is commonly diagnosed on the basis of imaging features alone without histological confirmation in the setting of cirrhosis. A multiphase contrast material-enhanced study is used (either CT or MR imaging) to set the radiologic diagnosis of HCC. The nodules that are suspicious for HCC during surveillance are new nodules that measure more than 1 cm or nodules that enlarge over a time interval. Following hepatocarcinogenesis, regenerative nodule dedifferentiates to dysplastic nodules and then to hepatocellular carcinoma. The vascular supply of HCC is mainly arterial though neoangiogenesis supplied by abnormal, unpaired hepatic arteries. Characteristically, HCC enhances during the arterial phase because of its blood supply. In the portal venous and equilibrium phase, the surrounding liver parenchyma becomes relatively hypoattenuated, and the lesion is perceived to be hypoattenuated because of its lack of portal venous supply corresponding to the so-called washout effect (Fig. 21.2). The third characteristic feature is pseudocapsule enhancement in the equilibrium phase. The diagnosis of HCC can be made from a single imaging study when this characteristic enhancement patterns—that is, arterial phase hyperenhancement and venous or delayed phase washout—are present. These noninvasive criteria can only be applied to cirrhotic patients [14]. About 70% of HCCs show these characteristic enhancement features of hypervascular HCCs, while the other 30% either do not show washout appearance or are hypovascular HCCs. When looking at HCCs 1 cm in size or less, only about 47% show typical enhancement features. When using Gd-EOB-DTPA, about 90% demonstrate hypointensity on hepatobiliary phase images and 10% demonstrate iso- or hyperintensity. Especially in hypovascular HCCs, which are difficult to diagnose with extracellular contrast agents, the hepatocyte-specific contrast agent (Gd-EOB-DTPA) is useful. Among the hypovascular HCCs,

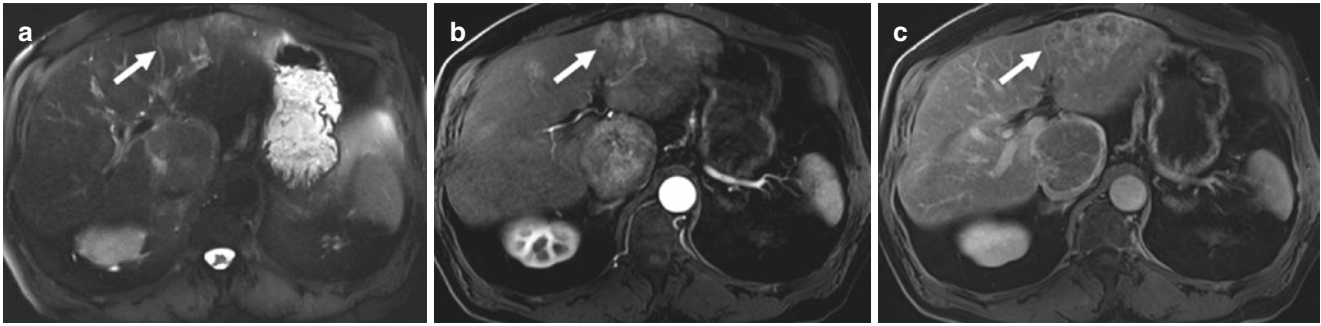


**Fig. 21.2** Multifocal HCC. 69-year-old patient with biopsy-proven metabolic toxic liver cirrhosis. (a) Axial T2-weighted magnetic resonance image demonstrates an iso- to slightly hyperintense lesion in the caudate lobe and multiple confluent lesions in the left liver lobe (white

arrow) with early enhancement in the arterial phase (b) and washout with peripheral enhancement (pseudocapsule appearance) in the equilibrium phase (c). With the typical appearance, the lesions can be categorized as LI-RADS 5 lesions

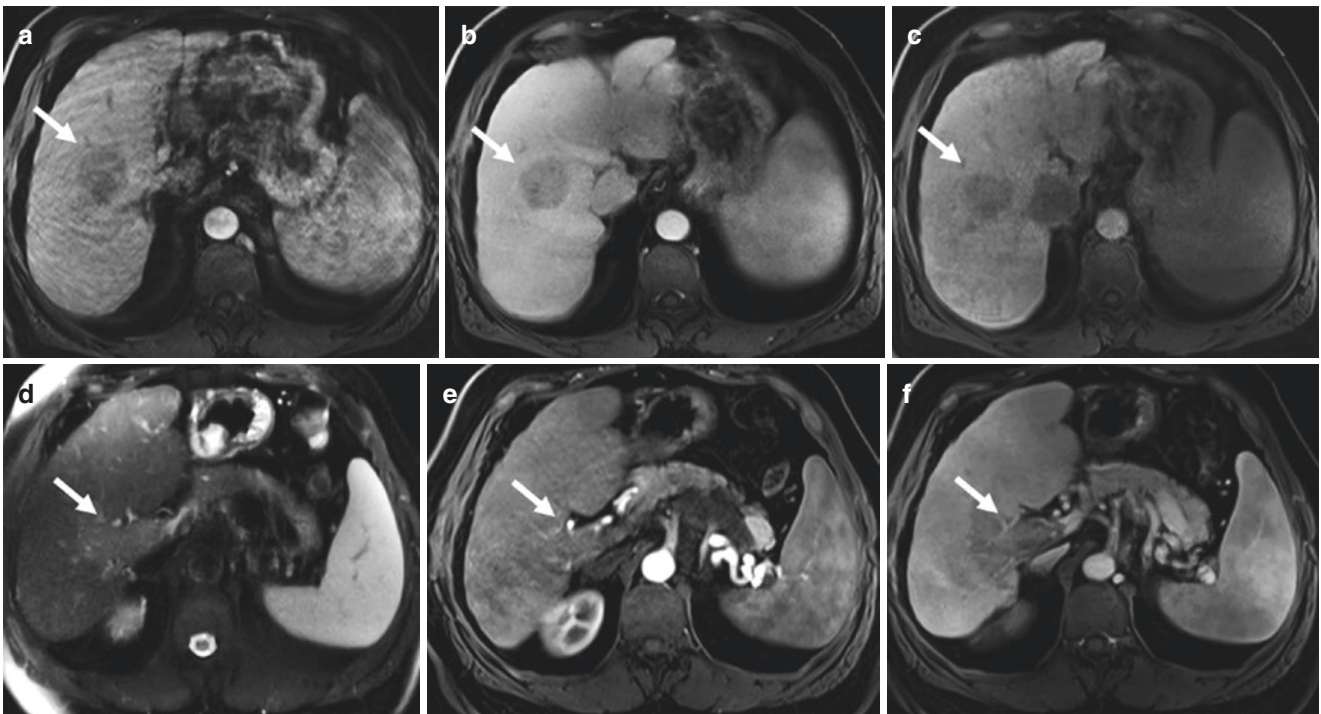


**Fig. 21.3** Hypovascular HCC. 60-year-old male patient with chronic hepatitis B and Child C cirrhosis. Initial imaging study (a–c) showed a focal hypovascular lesion (arrow) in liver segment 5 and 8 without contrast enhancement (Gd-EOB-DTPA) in the arterial (a), portal venous

(b), and hepatocyte-specific phase (c) consistent with an atypical hypovascular HCC. No treatment was performed, and the follow-up study 3 months later (d–f) shows progression of the tumor (arrow) with invasion into the portal vein

97% demonstrate hypointensity on hepatobiliary phase images (Fig. 21.3) [15]. In dynamic phases the contrast enhancement of typical, hypervascular HCCs with hepatocyte-specific contrast agent is comparable to extracellular contrast agents. In delayed phase (2–4 min after contrast administration), the washout may appear more pronounced because the surrounding liver parenchyma progressively takes up the contrast agent. The pseudocapsule appearance may be less visible due to background liver enhancement.

#### 21.2.4 Cholangiocellular Carcinoma

Intrahepatic cholangiocellular carcinoma (ICC) is the second most common primary hepatic tumor and accounts for 10–20% of all primary hepatic tumors. Recently, cirrhosis and viral hepatitis C and B have been recognized as risk factors for cholangiocarcinoma, especially for the intrahepatic type [16]. Radiologic features of cholangiocarcinoma such as progressive contrast enhancement from arterial to venous and late phase and arterial or both arterial and venous rim

enhancement can help differentiate ICC from HCC in the cirrhotic liver [17] (Fig. 21.4). Mixed hepatocellular cholangiocarcinoma has emerged as a distinct subtype of primary liver cancer [16, 18]. A strong enhancing rim and irregular shape on gadoxetic acid-enhanced MRI favors mixed hepatocellular-cholangiocellular carcinoma, and lobulated shape, weak rim and targeted appearance favors a mass-forming intrahepatic cholangiocarcinoma [16, 19].

### 21.2.5 Standardized Reporting Approach

Given the spectrum of focal liver lesions in stepwise hepatocarcinogenesis ranging from regenerative nodules to poorly differentiated HCC and the overlap in imaging features between the different steps, a definite diagnosis of a benign or malignant lesion in the cirrhotic liver is often not possible. Furthermore, a great variety in nomenclature of imaging features of cirrhotic nodules is used. To overcome these difficulties, the Liver Imaging Reporting and Data System (LI-RADS) has recently been developed, which is a comprehensive system for standardized interpretation and reporting of computed tomography (CT) and magnetic resonance (MR) examinations performed in patients at risk for HCC. It uses a standardized nomenclature and provides a diagnostic algorithm that uses imaging features to categorize the observations seen in patients at risk for HCC along a spectrum

from benign to malignant. Liver lesions in these patients are rated for their risk of being an HCC. LI-RADS 1 category observations are those that demonstrate imaging features diagnostic of a benign entity, e.g., cyst and hemangioma. LI-RADS 2 category observations are those that are probably benign, such as a hemangioma with an atypical enhancement pattern or a probably benign cirrhotic nodule. Major features including arterial-phase enhancement, lesion diameter, washout appearance, capsule appearance, and threshold growth are imaging features used to categorize LI-RADS 3 (indeterminate probability of HCC), LI-RADS 4 (probably HCC), and LI-RADS 5 (definitely HCC) lesions. LI-RADS 5 lesions have typical imaging features diagnostic for HCC (Fig. 21.2) [20].

## 21.3 Diffuse Vascular Liver Disease

### 21.3.1 Arteriovenous Shunts

Intrahepatic arteriportal shunts are communications between the hepatic arterial system and a portal vein or between hepatic arteries and hepatic veins which can be either at the level of the trunk, sinusoids, or peribiliary venules. In a cirrhotic liver, they can occur spontaneously, represent pseudolesions, and subsequently resolve. Secondary shunts may be posttraumatic, postbiopsy, or

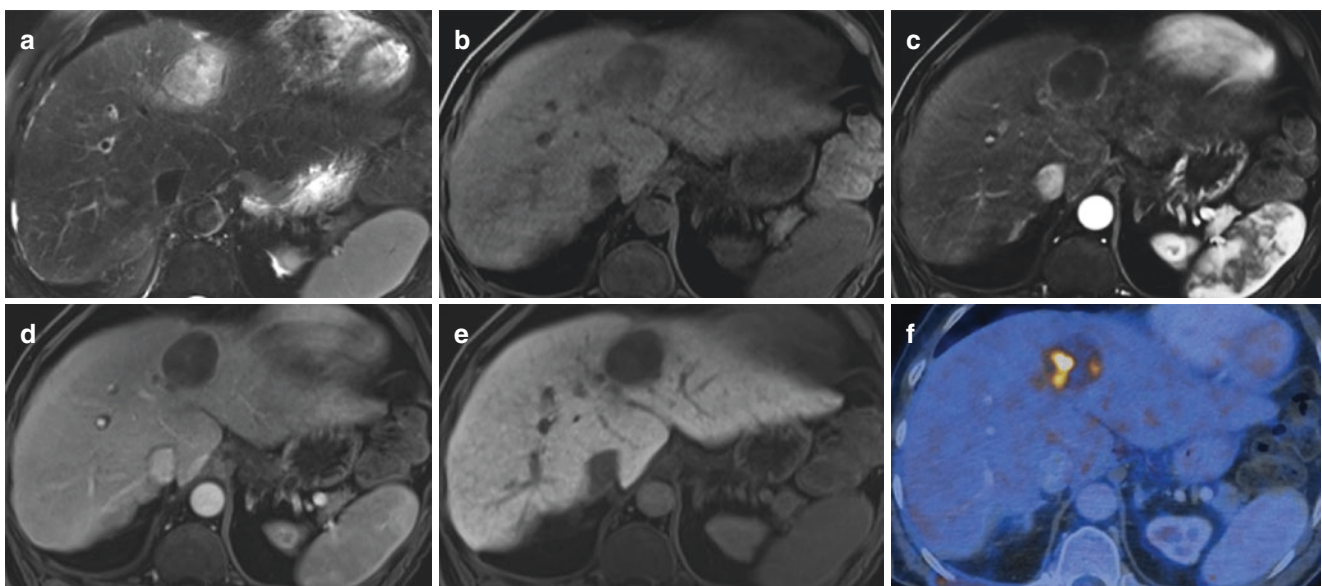


**Fig. 21.4** Cholangiocellular carcinoma in cirrhosis. 63-year-old male patient with chronic hepatitis C and Child A cirrhosis. (a) Axial T2-weighted magnetic resonance (MR) image shows features of cirrhosis with a focal hyperintense mass in the liver segment 2/4a with inhomogeneous signal intensity. (b–e) Corresponding axial gradient-echo T1-weighted images acquired before and after administration of hepatocyte-specific contrast agent (Gd-EOB-DTPA): (b) on pre-

contrast image, the lesion is hypointense; (c) in the arterial phase, the lesion shows rim enhancement, which persists in the portal venous phase (d); (e) in hepatocyte-specific phase, the lesion is hypointense. (f) Axial-fused image of fluoro-18-deoxyglucose (FDG) positron-emission tomography and computed tomography shows peripheral FDG uptake favoring cholangiocellular carcinoma over hepatocellular carcinoma, which was histologically confirmed

instrumentation. On imaging they appear as small, peripheral, nonspherical enhancing foci, which become isoattenuating to the liver in the portal venous phase. It may be difficult to distinguish an arterioportal shunt from a small hepatocellular carcinoma. Repeating imaging after 6 months usually helps distinguishing these entities and demonstrates resolution or stability of an arterioportal shunt or growth of an HCC.

### 21.3.2 Portal Venous Thrombosis

A thrombus in the portal vein can be either bland or through venous invasion from adjacent malignancies. Several causes lead to thrombosis of the portal vein system such as cirrhosis, hypercoagulable states, trauma, or abdominal tumors [21]. Disruption of the portal venous endothelium can occur in intra-abdominal inflammatory processes such as chronic inflammatory bowel disease, schistosomiasis, and pylephlebitis leading to portal venous thrombosis [11]. After acute occlusion numerous periportal collaterals can develop within 6–20 days even if partial recanalization of the thrombus develops, representing cavernous transformation of the portal vein [22] (Fig. 21.5), also known as portal cavernoma (PC). At ultrasound it appears as a mass of veins in the porta hepatis with hepatopetal flow that lacks the normal respiratory variation of the portal vein [21, 22]. PC represents a portoportal collateral pathway that substitutes for a thrombosed portal vein. The veins are usually insufficient to bypass the entire splenomesenteric inflow, and signs of portal hypertension such as splenomegaly frequently coexist [23]. On contrast-enhanced CT or MR scans, inhomoge-

neous, peripheral, patchy areas of high attenuation can be seen during the hepatic arterial phase. This pattern of perfusion occurs because the central regions of the liver are better supplied by the cavernous portal vein than are the peripheral regions; therefore, a peripheral increase in arterial inflow develops [23]. Portal biliopathy (PB) is defined as the presence of biliary abnormalities in patients with non-cirrhotic/nonneoplastic extrahepatic portal vein obstruction (EHPVO) and PC (Fig. 21.5). The pathogenesis of PB is due to the compression of bile ducts by PC and/or to ischemic damage secondary to an altered biliary vascularization in EHPVO and PC [24].

### 21.3.3 Budd-Chiari Syndrome

Budd-Chiari syndrome is defined as lobar or segmental hepatic venous outflow obstruction at the level of the inferior vena cava (IVC, type 1) or at the level of the hepatic veins (type 2) or occlusion of small centrilobular veins (type 3). Primary causes include congenital causes such as webs and diaphragms, outflow obstruction at the level of the right atrium, injury, and infection. Rarely the outflow obstruction may be due to mass effects from hepatic mass-forming malignancies. Secondary causes most commonly are thrombotic including obstruction after chemotherapy or radiation and hypercoagulability state due to oral contraceptive use, pregnancy, or polycythemia. The imaging findings are variable and depend on the disease state. Characteristic findings include hepatic venous outflow obstruction. In the acute state, the IVC and/or hepatic veins may appear hyperattenuating on unenhanced CT images because of the increased attenuation

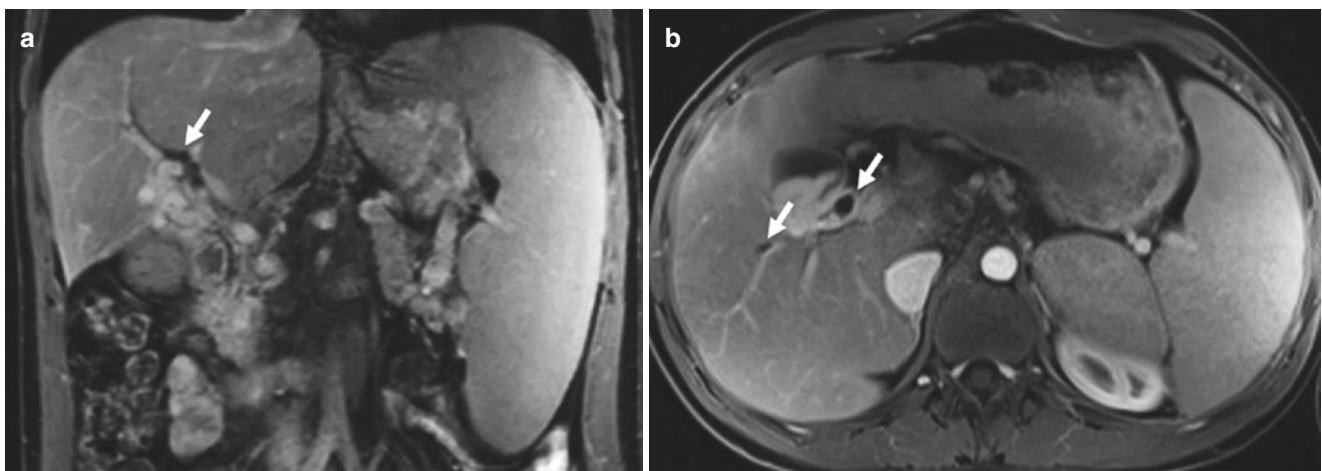


**Fig. 21.5** Chronic portal venous thrombosis with cavernous transformation. 16-year-old male patient with Faktor-V-Leiden mutation and history of omphalitis with portal vein thrombosis since infancy. Coronal (a) and axial (b) T1-weighted contrast-enhanced magnetic resonance (MR) images in the portal venous phase demonstrate cavernous trans-

formation of the portal vein with serpentine-like vessels in the porta hepatis and splenomegaly. In addition, dilated intra- and extrahepatic bile ducts (arrows) are noted caused by stenosis of the distal hepatocholangial duct probably due to the varices in the porta hepatis (the so-called portal biliopathy)

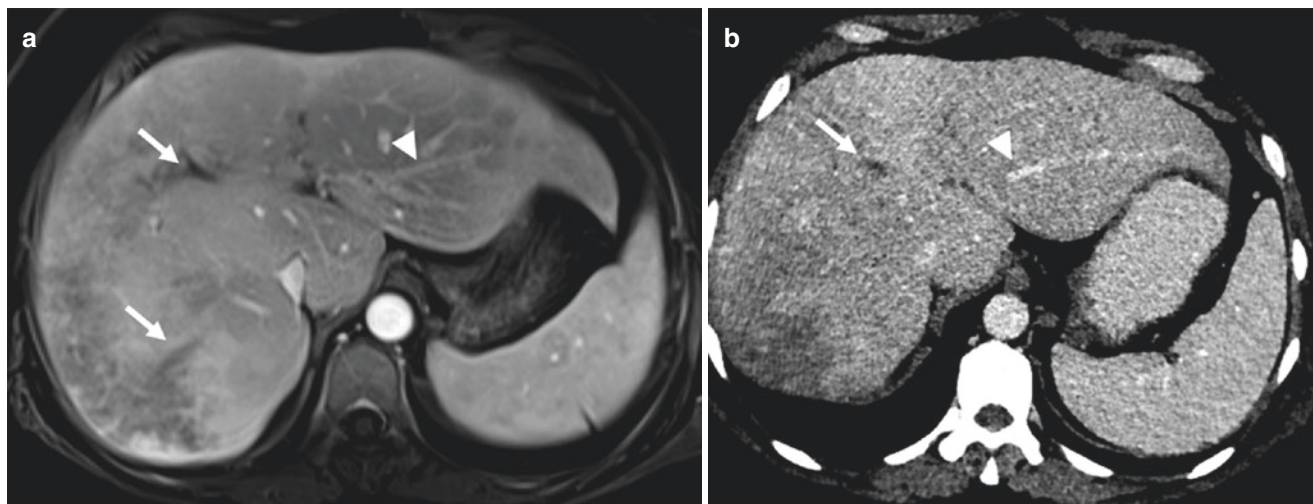


**Fig. 21.6** Budd-Chiari syndrome. 48-year-old female patient with chronic primary immunothrombocytopenia. (a) Axial T1-weighted magnetic resonance image in portal venous phase and (b) axial CT image in portal venous phase show a filling defect in the thrombosed

middle and right hepatic vein (arrow) and normal left hepatic vein (arrow head). (a, b) Diminished peripheral contrast enhancement is seen in the right liver lobe due to acute venous occlusion

of a thrombus. On contrast-enhanced CT or MRI, a vascular filling defects due to thrombotic material, reduction of hepatic vein caliber, missing connection between hepatic veins, and IVC can be present, or hepatic veins may not be visible at all. In the acute phase, diminished enhancement of the liver periphery and accentuated enhancement of central liver parts and caudate lobe are seen. Later on peripheral liver enhancement becomes heterogeneous as disorganized, comma-shaped intrahepatic collateral veins and systemic collateral veins develop. Large regenerative nodules in a dysmorphic liver are frequent findings in longer-standing venous outflow obstruction. These regenerative nodules appear hyperintense on hepatobiliary phase images after administration of a hepatocyte-specific contrast agent. Hypertrophy of the caudate lobe with variation in attenuation due to separate venous drainage should not be interpreted as a tumor [25]. Figure 21.6 shows an example of acute Budd-Chiari syndrome.

#### 21.3.4 Passive Hepatic Congestion

Passive hepatic congestion is due to chronic right-sided heart failure which leads to stasis of blood within the liver parenchyma. An enlarged, heterogeneous liver may be seen as a manifestation of acute or early cardiac disease. Early arterial enhancement of the dilated IVC and central hepatic veins is caused by reflux of contrast material from the right atrium into the IVC. A heterogeneous, mottled mosaic pattern of enhancement is present in the parenchymal phase, a condition also known as “nutmeg” liver. In long-standing disease, progressive cellular necrosis results in a small cirrhotic liver.

#### Key Points

- MR elastography can accurately diagnose clinically significant hepatic fibrosis.
- Hypovascular cirrhotic nodules with hypointense appearance on hepatobiliary phase images carry a significant risk of transformation into a hypervascular HCC.
- The diagnosis of HCC in cirrhotic patients can be made from a single imaging study when characteristic enhancement patterns—that is, arterial phase hyperenhancement and venous or delayed phase washout—are present.
- The presence of arterial or both arterial and venous rim enhancement can help differentiate intrahepatic cholangiocarcinoma from HCC in the cirrhotic liver.
- LI-RADS provides a diagnostic algorithm that uses imaging features to categorize the observations seen in patients at risk for HCC along a spectrum from benign to malignant.
- It may be difficult to distinguish an arteriportal shunt from a small hepatocellular carcinoma. Repeating imaging after 6 months usually helps distinguishing these entities.
- Budd-Chiari syndrome is a heterogeneous group of disorders characterized by hepatic venous outflow obstruction at the level of the hepatic veins, the inferior vena cava (IVC), or the right atrium [26].

## References

- Dulai PS, Sirlin CB, Loomba R. MRI and MRE for non-invasive quantitative assessment of hepatic steatosis and fibrosis in NAFLD and NASH: clinical trials to clinical practice. *J Hepatol*. 2016;65(5):1006–16.
- Permutt Z, Le TA, Peterson MR, et al. Correlation between liver histology and novel magnetic resonance imaging in adult patients with non-alcoholic fatty liver disease—MRI accurately quantifies hepatic steatosis in NAFLD. *Aliment Pharmacol Ther*. 2012;36(1):22–9.
- Tang A, Tan J, Sun M, et al. Nonalcoholic fatty liver disease: MR imaging of liver proton density fat fraction to assess hepatic steatosis. *Radiology*. 2013;267(2):422–31.
- Idilman IS, Aniktar H, Idilman R, et al. Hepatic steatosis: quantification by proton density fat fraction with MR imaging versus liver biopsy. *Radiology*. 2013;267(3):767–75.
- Singh S, Venkatesh SK, Wang Z, et al. Diagnostic performance of magnetic resonance elastography in staging liver fibrosis: a systematic review and meta-analysis of individual participant data. *Clin Gastroenterol Hepatol*. 2015;13(3):440.e6–51.e6.
- Loomba R, Wolfson T, Ang B, et al. Magnetic resonance elastography predicts advanced fibrosis in patients with nonalcoholic fatty liver disease: a prospective study. *Hepatology*. 2014;60(6):1920–8.
- Kim D, Kim WR, Talwalkar JA, Kim HJ, Ehman RL. Advanced fibrosis in nonalcoholic fatty liver disease: noninvasive assessment with MR elastography. *Radiology*. 2013;268(2):411–9.
- Yoon JH, Lee JM, Joo I, et al. Hepatic fibrosis: prospective comparison of MR elastography and US shear-wave elastography for evaluation. *Radiology*. 2014;273(3):772–82.
- Ichikawa S, Motosugi U, Morisaka H, et al. Comparison of the diagnostic accuracies of magnetic resonance elastography and transient elastography for hepatic fibrosis. *Magn Reson Imaging*. 2015;33(1):26–30.
- Brancatelli G, Federle MP, Ambrosini R, et al. Cirrhosis: CT and MR imaging evaluation. *Eur J Radiol*. 2007;61(1):57–69.
- Hodler JK-HR, von Schulthess GK, Zollner CL. *Diseases of the abdomen and pelvis 2014–2017*. Milan: Springer; 2014.
- Parente DB, Perez RM, Eiras-Araujo A, et al. MR imaging of hypervascular lesions in the cirrhotic liver: a diagnostic dilemma. *Radiographics*. 2012;32(3):767–87.
- Suh CH, Kim KW, Pyo J, Lee J, Kim SY, Park SH. Hypervascular transformation of Hypovascular Hypointense nodules in the Hepatobiliary phase of Gadoxetic acid-enhanced MRI: a systematic review and meta-analysis. *AJR Am J Roentgenol*. 2017;209(4):781–9.
- McEvoy SH, McCarthy CJ, Lavelle LP, et al. Hepatocellular carcinoma: illustrated guide to systematic radiologic diagnosis and staging according to guidelines of the American Association for the Study of Liver Diseases. *Radiographics*. 2013;33(6):1653–68.
- Choi JW, Lee JM, Kim SJ, et al. Hepatocellular carcinoma: imaging patterns on gadoxetic acid-enhanced MR images and their value as an imaging biomarker. *Radiology*. 2013;267(3):776–86.
- Razumilava N, Gores GJ. Cholangiocarcinoma. *Lancet*. 2014;383(9935):2168–79.
- Huang B, Wu L, Lu XY, et al. Small intrahepatic Cholangiocarcinoma and hepatocellular carcinoma in cirrhotic livers may share similar enhancement patterns at multiphase dynamic MR imaging. *Radiology*. 2016;281(1):150–7.
- Komuta M, Govaere O, Vandecaveye V, et al. Histological diversity in cholangiocellular carcinoma reflects the different cholangiocyte phenotypes. *Hepatology*. 2012;55(6):1876–88.
- Chong YS, Kim YK, Lee MW, et al. Differentiating mass-forming intrahepatic cholangiocarcinoma from atypical hepatocellular carcinoma using gadoxetic acid-enhanced MRI. *Clin Radiol*. 2012;67(8):766–73.
- Santillan CS, Tang A, Cruite I, Shah A, Sirlin CB. Understanding LI-RADS: a primer for practical use. *Magn Reson Imaging Clin N Am*. 2014;22(3):337–52.
- Elsayes KM, Shaaban AM, Rothan SM, et al. A comprehensive approach to hepatic vascular disease. *Radiographics*. 2017;37(3):813–36.
- De Gaetano AM, Lafortune M, Patriquin H, De Franco A, Aubin B, Paradis K. Cavernous transformation of the portal vein: patterns of intrahepatic and splanchnic collateral circulation detected with Doppler sonography. *AJR Am J Roentgenol*. 1995;165(5):1151–5.
- Gallego C, Velasco M, Marcuello P, Tejedor D, De Campo L, Frieria A. Congenital and acquired anomalies of the portal venous system. *Radiographics*. 2002;22(1):141–59.
- Franceschet I, Zanetto A, Ferrarese A, Burra P, Senzolo M. Therapeutic approaches for portal biliopathy: a systematic review. *World J Gastroenterol*. 2016;22(45):9909.
- Torabi M, Hosseinzadeh K, Federle MP. CT of nonneoplastic hepatic vascular and perfusion disorders. *Radiographics*. 2008;28(7):1967–82.
- Ludwig J, Hashimoto E, McGILL DB, van HEERDEN JA. Classification of hepatic venous outflow obstruction: ambiguous terminology of the Budd-Chiari syndrome. *Mayo Clinic Proceedings*; Elsevier; 1990. p. 51–5.

**Open Access** This chapter is licensed under the terms of the Creative Commons Attribution 4.0 International License (<http://creativecommons.org/licenses/by/4.0/>), which permits use, sharing, adaptation, distribution and reproduction in any medium or format, as long as you give appropriate credit to the original author(s) and the source, provide a link to the Creative Commons license and indicate if changes were made.

The images or other third party material in this book are included in the book's Creative Commons license, unless indicated otherwise in a credit line to the material. If material is not included in the book's Creative Commons license and your intended use is not permitted by statutory regulation or exceeds the permitted use, you will need to obtain permission directly from the copyright holder.

